Available online at www.sciencedirect.com
SCIENCE DIRECT®
Methods 34 (2004) 408–414
METHODS
www.elsevier.com/locate/ymeth

Crystallization of RNA and RNA–protein complexes

Ailong Ke[a] and Jennifer A. Doudna[a,b,*]

[a] *Department of Molecular and Cell Biology and Department of Chemistry, University of California, Berkeley, Berkeley, CA 94720, USA*
[b] *Howard Hughes Medical Institute, University of California, Berkeley, Berkeley, CA 94720, USA*

Accepted 24 March 2004

Abstract

RNA plays a direct role in a variety of cellular activities, and in many cases its biological function is conferred by the RNA three-dimensional structure. X-ray crystallography is the method of choice for determining high resolution structures of large RNA molecules, and can also be used to compare related RNAs and identify conformational changes that may accompany biochemical activity. However, crystallization remains the rate-limiting step in RNA structure determination due to the difficulty in obtaining well-ordered crystals for X-ray diffraction analysis. Several approaches to sample preparation, crystallization, and crystal handling are presented that have been used successfully in the structure determination of RNA and RNA–protein complexes in our laboratory, and should be generally applicable to RNAs in other systems.

Keywords: RNA; Ribozyme; Crystallization; RNP

1. Introduction

The explosion of interest in RNA and RNA–protein complexes in recent years stems from the discovery that RNA plays much more varied roles in biology than had previously been suspected. In addition to its long-recognized participation in all aspects of protein biosynthesis, structured RNA molecules are also central to the activities of ribonucleoprotein complexes responsible for telomere replication, X-chromosome inactivation, protein trafficking, and RNA splicing and processing. In addition, RNA interference involves hundreds of small RNA oligonucleotides that are processed from larger precursors and inactivate specific messenger RNAs by mechanisms whose details have yet to be elucidated. Along with the increased interest in RNA biology has come the recognition that understanding RNA activities will require knowledge of the structures and conformational dynamics of these molecules. The crystal structures of ribozymes and of the ribosome and its subunits solved in the past few years have revealed many of the principles that enable RNA helices to pack into compact three-dimensional structures that create catalytic centers and ligand binding sites. Nonetheless, much remains to be learned about RNA that can only be revealed in detail by X-ray crystal structure determination. This review outlines a variety of methods used to prepare and crystallize RNA samples and optimize crystals for X-ray diffraction analysis, with examples from experience in our own laboratory.

2. Principles of RNA crystallization

Crystallization is predictably the least predictable aspect of a structure determination project. Many factors affect the inherent crystallizability of an RNA sample, including purity, conformational homogeneity, molecular surface area, and available sites for intermolecular contacts, ligand binding, and structural dynamics. A crystal is a well-ordered three-dimensional array of molecules held together by non-covalent interactions called "crystal contacts." In general, crystals of

* Corresponding author. Fax: 1-510-643-0080.
E-mail address: doudna@uclink.berkeley.edu (J.A. Doudna).

1046-2023/$ - see front matter © 2004 Elsevier Inc. All rights reserved.
doi:10.1016/j.ymeth.2004.03.027

nucleic acids and proteins can be grown by slow, controlled precipitation from aqueous solution under non-denaturing conditions. Among the various crystallization techniques available, the most popular are hanging/sitting drop vapor diffusion and microbatch. The former involves applying 1–10 μl of crystallization sample onto a platform (sitting drop) or an inverted glass cover slide (hanging drop) and allowing it to equilibrate against a much larger volume (0.5 ml or more) of reservoir solution through vapor diffusion in a sealed environment. The latter involves mixing samples with crystallization reagents and allowing the drop to equilibrate with air through a layer of oil. Both methods are successful in identifying initial crystallization conditions, while sample volumes as small as 20 nl can be set up in automated fashion using the microbatch method, enabling high-throughput crystal screening ([1] and references therein). A promising new method using microfluidics, described in this volume of Methods (S. Quake article), enables screening of 48 crystallization conditions, each at three sample-to-precipitant ratios, with just 3 μl of sample.

Despite these approaches, obtaining well-ordered crystals is still seemingly more difficult for RNA and RNA–protein complexes than for proteins. Several factors may contribute to this. Whereas proteins can utilize a large number of structural and chemical features on their molecular surface to form crystal contacts, the repetitive array of negatively charged phosphate groups on the surface of an RNA molecule makes crystal packing more difficult and potentially error-prone. Hence, many nucleic acid crystals are poorly ordered and diffract X-rays to only low resolution [2]. Unlike most proteins that fold into globular domains, RNAs frequently adopt elongated shapes that pack loosely in crystals, with high solvent content. Furthermore, the relatively weak tertiary interactions within RNA molecules lead to more flexibility and inter-domain movements, and a higher tendency to misfold. The former results in weaker diffraction and higher temperature factors in RNA crystals, while the latter leads to non-homogeneous samples that are hard to crystallize.

Because of these problems, active engineering can be very useful for obtaining diffraction quality crystals (for reviews, see [3–5]). A blunt or "sticky" end may be engineered into RNA to promote inter-molecular stacking interactions that form "super helices" in the crystal lattice [6]. Non-essential regions within the RNA may be deleted or replaced with stem loops that may potentially form specific crystal contacts. For example, GNRA tetraloops and cognate receptor sequences were found to mediate crystal contacts in hammerhead ribozyme crystals [7,8]. Engineering GAAA tetraloop–tetraloop receptor interactions into non-essential regions of the hepatitis delta virus (HDV) ribozyme yielded many more crystal forms than controls [2]. A similar engineering approach produced crystals diffracting to 1.5 Å resolution for the Ffh M-domain bound to 4.5S RNA [9]. Another successful approach involves engineering the U1A binding site sequence into non-essential regions of the RNA, and crystallizing the RNA in complex with the U1A RNA binding domain (RBD) protein. This approach dramatically improved the crystallizability of the HDV and hairpin ribozymes [10–12]. The rigid, positively charged U1A protein serves as a structural landmark and forms most of the contacts in the HDV ribozyme crystal lattice, significantly increasing the diffraction limit of the ribozyme crystals [10]. The structure determination process is also expedited by preparing Se-derivatized U1A protein and using multiwavelength anomalous diffraction (MAD) to solve the phase problem [11,12]. Crystallization modules are usually introduced into an RNA molecule through a helical adaptor segment, whose length can be systematically varied to allow those modules to sample different orientations [2].

Another successful approach to improving the quality of RNA crystals has been to use in vitro selection to identify more stable folding variants of a native molecule. Crystals of the P4–P6 domain of the *Tetrahymena* group I intron were improved by selection of a P4–P6 mutant that folds at a lower magnesium ion concentration than the native sequence [13,14]. To overcome an apparent flexibility problem that prevented crystals of the *Tetrahymena* self-splicing group I intron from diffracting to high resolution, in vitro selection was used to identify active variants of the intron with increased thermal stability [15]. The melting temperature was increased 10.5 °C in the final selection product, which contains nine point mutations; most of these seem to improve intramolecular packing interactions in the molecular interior. This variant *Tetrahymena* intron self-cleaves to a greater extent, although at a slightly slowly rate, than the wild type [15]. Crystals of the *Tetrahymena* intron with a subset of these nine mutations introduced diffracted to 3.8 Å resolution, a significant improvement from 5.0 Å for the wild type crystals (personal communication, Dr. Feng Guo, University of Colorado at Boulder).

3. Sample preparation

Milligram quantities of RNA required for crystallization experiments can be obtained from two sources: chemical synthesis and in vitro run-off transcription using T7 RNA polymerase. Nucleotide modifications site-specifically incorporated during chemical synthesis can be exploited in structure determination and functional studies. However, there is an effective length limit of ~40 nucleotides for chemical synthesis, as abortive products accumulate with each cycle of nucleotide addition. Much larger RNAs can be generated by in vitro

transcription reactions. In this case, the RNA coding sequence is subcloned into a high-copy number plasmid such as pUC19 (New England Biolabs) under the control of a T7 RNA polymerase promoter. The construct is then amplified in bacterial cell culture, purified, and linearized at a restriction site engineered at the 3′ end of the coding sequence. The overall transcription yield is very sensitive to the sequence at the 5′ end of the product RNA, as T7 polymerase prefers one or more guanosines at the 5′ terminus [16,17]. The polymerase also randomly incorporates 1–3 nucleotides at the 3′ end of the transcript, generating N + 1, N + 2, and/or N + 3 extensions [16,17]. Self-cleaving ribozymes flanking the coding sequence can cleave the RNA transcript in *cis* to generate homogeneous 5′ and 3′ ends [18,19]. Hammerhead and HDV ribozymes are routinely used to generate RNAs with a non-guanosine 5′ end and a homogeneous 3′ end, respectively. These two ribozymes have minimal sequence preferences to define the cleavage site. The hammerhead ribozyme, however, must be redesigned to maintain essential base-pairings each time a new RNA construct is to be made [18,19].

As much as 40 mg of purified RNA can be produced from a 10 ml transcription reaction following a typical in vitro transcription protocol. It is important to optimize the Mg^{2+}, plasmid template, and T7 polymerase concentrations for each RNA construct to be used. A standard transcription reaction used to prepare RNA in sufficient quantity for a set of crystallization experiments consists of the following:

100 mM (NTPs)	500 μl of each
1 M Tris–HCl, pH 8.1	300 μl
1 M $MgCl_2$	250 μl
1 M DTT	100 μl
1% Triton X-100	100 μl
1 M spermidine	20 μl
Linearized plasmid	500 μg
DEPC-H_2O	fill to 9 ml
Escherichia coli or yeast inorganic pyrophosphatase (1 U/μl)	10 μl
T7 RNA polymerase (1 mg/ml)	1 ml

The in vitro transcribed or chemically synthesized RNAs are routinely gel-purified under denaturing conditions. As much as 6 ml of RNA sample (mixed with 6 ml of 2× RNA loading buffer containing 80% (w/v) deionized formamide, 10 mM EDTA (pH 8.0)) can be applied and purified on a $24 \times 34 \times 0.3$ cm Tris/borate/EDTA (TBE) polyacrylamide gel containing 8 M urea. If only one major RNA product is expected, ~40 mg of RNA can be applied to one gel and purified away from plasmid template and abortive transcripts. If ribozymes are included in the transcript to process the ends of the RNA, care must be taken not to overload the gels such that separation of the desired RNA from the cleaved ribozymes is compromised. As a case in point, 2 mg of a 75-nucleotide precursor HDV ribozyme was separated from the cleaved product that is just three nucleotides shorter using a 10% $50 \times 34 \times 0.3$ cm denaturing gel; this material was used successfully in crystallization experiments. After electrophoresis, the RNA bands are identified by UV shadowing and the target RNA band is excised and crushed. RNA is eluted from the pulverized gel slices using DEPC-treated water, concentrated by three buffer exchanges using an Amicon concentrator, and stored at −80 °C until further use.

4. Large-scale RNA ligation to introduce modified nucleotides

The analysis of RNA crystal structures containing specifically incorporated modified nucleotides opens a new dimension in studying RNA structure–function relationships. For example, structures of self-cleaving ribozymes in the pre-cleavage state can be determined by replacing the 2′ hydroxyl of the attacking nucleotide with a 2′-deoxy,2′-methoxy or 2′-fluoro analog [7,11,20] (A.K. and J.A.D., unpublished). Time-resolved crystallography can, in principle, be carried out on ribozymes with a photolabile group such as *O*-nitrobenzyl attached to the 2′-oxygen at the active site [21]. The use of a methyl group adjacent to the 5′ oxygen leaving group of the hammerhead ribozyme created a kinetic bottleneck, trapping the in-line attacking conformation for crystallographic structure determination [22]. In addition, 5-bromo- or 5-iodo-uridine or cytidine is frequently incorporated into RNA to facilitate experimental phase determination [23,24].

To crystallize RNAs larger than ~40 nucleotides containing modifications, a short synthetic RNA is annealed with a larger unmodified transcript, leaving a nick in the phosphate backbone [23,25]. This approach limits the modifications to the 5′ or 3′ region of the RNA, and the resulting two-piece construct may affect the RNA conformation and activity. These problems can be solved by covalent ligation of the two RNAs using either T4 RNA ligase [26] or T4 DNA ligase [27]. Scaling up the ligation reaction to produce enough material for crystallization, however, has proven to be technically challenging.

We used large-scale RNA ligation to introduce 2′-deoxy (H) and 2′-methoxy (MeO) nucleotide modifications adjacent to the scissile phosphate in the HDV ribozyme, enabling crystallization and structure determination of the ribozyme in the pre-cleavage stage. The HDV precursor ribozyme was produced by splinted ligation of two RNA segments [28]. The 13-nt 5′ donor RNA oligonucleotide, containing a GAU trinucleotide leader sequence followed by the first 10 nucleotides of the ribozyme, was synthesized chemically at a 1 μmol scale with a 2′-H or 2′-MeO modification incorporated

preceding the labile phosphate. This RNA was desalted, deprotected, and used directly in the ligation reaction without further purification. The 62-nt acceptor RNA molecule containing the rest of the ribozyme was transcribed in vitro using T7 RNA polymerase. To ensure that the RNA transcript contained a monophosphate rather than a triphosphate at the 5′ end, 20 mM guanosine monophosphate (GMP) was included together with 1 mM guanosine triphosphate (GTP) in the in vitro transcription reaction. GMP can only be incorporated at the 5′ end of the RNA transcript, and the 20:1 ratio of GMP to GTP ensures that ~95% of the transcripts contain a monophosphate at the 5′ terminus. A DNA splint complementary to the entire donor RNA sequence as well as the first 20 nts of the acceptor sequence was chemically synthesized at a 1 μmol scale. Efficient ligation of RNA substrates requires an amount of purified T4 DNA ligase that is at least stoichiometric with substrate because this enzyme does not turn over efficiently on RNA-containing duplexes [28]. To circumvent the high cost of commercially available T4 DNA ligase, we used a plasmid encoding a $(His)_6$-tagged T4 DNA ligase (generous gift of Dr. Scott Strobel, Yale University) to produce 200 mg of ~95% pure T4 DNA ligase from 10 L of bacterial culture [29]. The purified ligase is highly active in splinted ligation reactions and contains negligible RNase or DNase activity.

The efficiency of splinted ligation reactions is highly dependent on the percentage of correctly annealed RNA donor/acceptor/DNA splint molecules. For this reason, ribozymes and other highly structured RNAs are not the best ligation substrates since they contain extensive secondary and tertiary folds that may prevent efficient splint hybridization. Various methods have been suggested to increase the ligation yield, including varying the ligation site, annealing the substrates, and splint sequentially, or including a "disrupter" DNA oligonucleotide to compete with RNA tertiary interactions [28]. Our initial attempts to anneal the RNA donor, acceptor, and DNA splint in equimolar concentrations resulted in less than 40% of correctly annealed RNA/DNA hybrid as judged by native polyacrylamide gel analysis, and the ligation efficiency was only 5–10% of the input sample. Including a disrupter DNA strand complementary to internal sequences in the ribozyme had little or no effect on the annealing and ligation efficiency. We reasoned that higher molar ratios of RNA donor and DNA splint to the structured acceptor RNA might drive the equilibrium toward formation of productive RNA/DNA hybrids during annealing. When the molar ratio of donor/splint/acceptor was changed to 2:1.5:1, the splinted ligation efficiency increased to over 90% (Fig. 1). The reaction time and temperature were further optimized, showing that 30 °C gives a better yield than 16 and 4 °C. In a time course experiment, the ligated RNA product began to

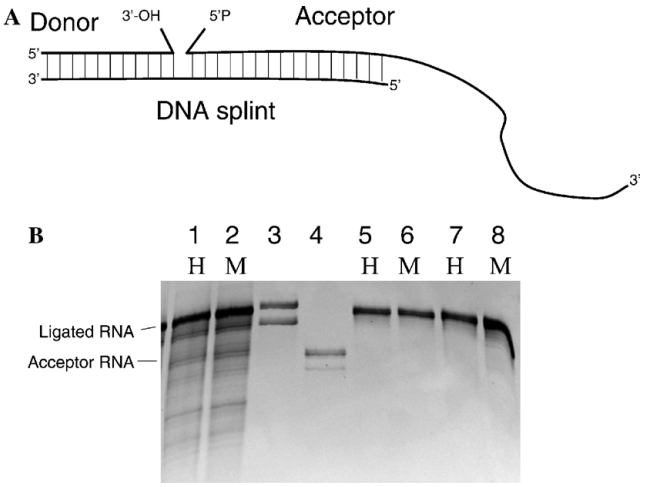

Fig. 1. (A) Diagram showing the design of a splinted ligation reaction. A donor and an acceptor RNA with 3′-OH and 5′-monophosphate termini, respectively, are annealed with a complementary DNA splint. The two RNA molecules are then joined covalently by incubation of the annealed complex with T4 DNA ligase. (B) Large scale splint-mediated ligation of two RNA molecules to generate the full-length HDV ribozyme construct. As shown in this ethidium-stained 10% urea–PAGE gel, a 62-nt in vitro transcribed RNA (lane 4) was covalently joined to a 13-nt modified RNA in a DNA splint-mediated ligation reaction to produce non-cleavable precursor HDV ribozyme (lane 1, RNA with 2′ deoxy (H) modification adjacent to scissile phosphate; lane 2, RNA with 2′-methoxy (M) modification at the same site). The modified RNAs were purified to homogeneity on a preparative-scale 10% urea–PAGE gel (lanes 5, 6). No apparent ribozyme cleavage activity was observed for the modified RNAs mixed with U1A-RBD protein and urea-refolded in the presence of 2.5 mM $MgCl_2$ (lanes 7 and 8). A mixture of 72-nt and 78-nt HDV ribozyme RNA was used as a molecular weight marker (lane 3).

accumulate within 30 min, reached a maximum between 5 and 7 h, and declined slightly after overnight incubation. A detailed splinted ligation procedure for 20 ml of RNA at 16 μM concentration is carried out as follows.

Annealing. To 8.2 ml of DEPC-treated H_2O, add 3.0 ml of 212 μM donor RNA, 2.3 ml of 138 μM acceptor RNA, 3.78 ml of 126 μM DNA splint, and 2.0 ml of 10× ligation buffer (660 mM Tris–HCl (pH 7.5), 66 mM $MgCl_2$, and 100 mM DTT). The reaction mixture is heated to 90 °C for 6 min, and cooled to 30 °C over the course of 2 h.

Ligation. To the annealed reaction, add 100 μl of 100 mM ATP and 620 μl of 500 μM T4 DNA ligase. The ligation reaction is allowed to proceed for 5 h at 30 °C.

Product purification. The ligation reaction is quenched by phenol/chloroform extraction; the nucleic acids are then ethanol precipitated, re-dissolved in 8 ml of 1× formamide gel loading buffer, and purified on a 10% denaturing polyacrylamide gel. From 6.7 mg of acceptor RNA input, we obtained 2.1 mg of pure ligated precursor HDV ribozyme with a 2′-H modification at the cleavage site.

5. Sample renaturation to induce conformational homogeneity

It is critical to ensure that chemically homogeneous RNA samples also adopt a homogeneous conformation, as structural heterogeneity leads to poorly ordered crystals or prevents crystallization entirely. A common practice to ensure conformational homogeneity is to heat-denature RNA samples and renature them over a shallow temperature gradient. While this method works well for crystallizing some RNAs, it is not effective for others, such as the precursor HDV ribozyme, that tend to misfold [30,31]. Only 30–50% of freshly transcribed HDV ribozymes fold correctly and undergo self-cleavage, and heat renaturation of the inactive HDV ribozyme does not lead to significantly more cleavage (A.K. and J.A.D., unpublished results). NMR spectra of the precursor HDV ribozyme also indicate that multiple conformations may be present [32]. Not surprisingly, no crystals were ever observed from RNA samples prepared using a heat-renaturation procedure.

An alternative RNA renaturation method, used less frequently, involves denaturing RNA or an RNA–protein complex with 8 M urea and refolding the sample by gradual dialysis into buffer lacking urea. Urea-mediated refolding was used to overcome excessive RNA dimerization of the U2A'/U2B"/U2snRNA complex [33]. It was also critical for obtaining diffraction quality crystals of the M domain of Ffh protein bound to the core of 4.5S RNA [9]. In addition, the *Tetrahymena thermophila* group I intron has been shown to evade kinetic traps more efficiently in the presence of low urea concentrations [34,35]. The self-cleavage rate of the HDV ribozyme is enhanced 50-fold in the presence of 5 M Urea [36]. Using urea-mediated refolding, the precursor HDV ribozyme/U1A protein complex was crystallized in multiple conditions in the first round of a crystallization screen, and optimized crystals ultimately diffracted X-rays to a resolution of 2.1 Å. A detailed urea-mediated refolding protocol is as follows: The sample (in our case, the precursor HDV ribozyme RNA complexed with U1A protein) at 0.5 mM concentration is diluted into 9 volumes of denaturing buffer A (25 mM Tris–HCl, pH 7.5, 20 mM NaCl, and 2.5 mM $MgCl_2$) and 8 M urea. After overnight dialysis against this buffer at 4 °C, the complex is transferred in three 3-h dialysis steps into buffer A containing decreasing urea concentrations of 4, 2, and 0 M, respectively, and reconcentrated to 0.5 mM using a Millipore microcon concentrator. By replacing 2.5 mM $MgCl_2$ in the renaturing buffer with 20 mM EDTA, the wild type HDV ribozyme self-cleavage activity could be effectively suppressed and was refolded by the same procedure. Ultrapure urea from Sigma is used in the above procedure to avoid trace metal contaminants that might trigger ribozyme cleavage.

6. Crystallization conditions and screening methods

RNA samples for crystallization should be transferred into a solution containing 10–20 mM buffer and a minimum amount of monovalent and divalent salts required for activity, and concentrated to ~0.5 mM. Before subjecting RNA samples to crystal screening, functional or enzymatic assays should be performed to ensure the RNA is fully active. For RNA–protein complexes, a molar RNA:protein ratio of 1:0.9 seems to work well for initial screening, guided by gel shift assays to ensure complete complex formation. Protein samples used should be verified to be free of RNase contamination by incubating with RNA at room temperature for several days; most (>95%) of the RNA should survive this treatment.

Several different "sparse matrix" crystallization screens have been published that allow one to search for RNA or RNA–protein complex crystallization conditions efficiently [37–41]. The commercially available Natrix and Nucleic Acid Mini screens from Hampton Research were used successfully in obtaining crystals of the HDV precursor ribozyme. Important variables explored in these crystal screens include the identity and concentration of divalent metal ions, polyamines such as spermine, spermidine, putrescine, metal hexamines, and pH. The most successful precipitants are 2-methyl-2,4-pentanediol (MPD) and polyethylene glycols (PEGs). Any positive "hits" in initial crystal screens, often manifested as tiny rods, needles or needle clusters, or thin plates, should be optimized by systematic variation of each parameter of the initial crystallization condition until large crystals (>100 μm in each dimension) can be obtained reproducibly (but see also the chapter by S. Quake on crystallization using microfluidic devices). Microseeding and macroseeding are frequently used to increase the size of initial crystals [42].

7. Crystal handling and cryo-stabilization

RNA and RNA–protein complex crystals tend to decay rapidly when exposed to X-rays. Thus, diffraction data are generally measured at cryogenic temperatures. Selection of a suitable cryoprotectant that enables cryogenic cooling without ice formation or damage to the crystal usually involves some trial and error. The most popular cryoprotectants include glycerol, MPD, PEGs, sugars such as sucrose, and volatile alcohols such as ethanol or isopropanol. Crystals are usually transferred stepwise into a synthetic mother liquor containing increasing concentrations of the cryoprotectant. The mother liquor is usually similar to the precipitating solution, with ionic strength and precipitant concentration adjusted to prevent cracking or dissolution of the crystal. Some of the mentioned cryoprotectants may be present

as the precipitating agent in a crystallization condition, and if so should be tested first. A cryoprotectant kit containing 36 cryo-solutions is sold by Hampton Research, facilitating a systematic search. When heavy atoms are to be introduced into crystals for experimental phase determination, the overall ionic strength and divalent ion concentrations should be kept as low as possible. This sometimes means a complete solvent exchange from high salt solutions to organic solvents such as MPD or PEG. Whenever possible, a crystal should be capillary-mounted in the X-ray beam to check the diffraction limit and mosaicity prior to cryoprotectant screening. The ultimate measure of cryoprotection success is good diffraction with minimum increase in crystal mosaicity.

Crystals with high solvent content tend to diffract X-rays weakly. Sometimes the diffraction limit can be improved by "crystal dehydration" ([43] and references therein). A simple process that has given good results in our laboratory is the following: The crystal is first transferred stepwise into 5 μl of mother liquor with increasing concentration of cryoprotectant. The drop containing the crystal is then covered with 20 μl paraffin oil (purchased from Hampton Research and dehydrated for one hour in a SpeedVac) and allowed to equilibrate with air for 1 h to overnight. In one case, this procedure produced more isomorphous crystals and improved the diffraction resolution from 3.2 to 2.1 Å.

8. Application to structure determination of the hepatitis delta virus ribozyme

In this section, we describe the crystallization process for the precursor HDV ribozyme. Found as two closely related genomic and antigenomic variants, the HDV ribozyme catalyzes efficient site-specific cleavage of the viral RNA phosphodiester backbone through transesterification [44]. This ribozyme has a non-specific requirement for divalent cations, and a cytidine nucleotide within the ribozyme sequence is essential to catalytic activity. The crystal structure of the product form of the HDV ribozyme [12] provided important insight into the cleavage mechanism of this ribozyme. However, knowledge of the precursor structure is essential to elucidate the role of divalent ions and the catalytically important cytidine residue. Crystallization of the precursor ribozyme was hampered by two technical difficulties: (1) There is inherent conformational heterogeneity in the precursor RNA samples due to misfolding; (2) It is difficult to trap the HDV ribozyme in the pre-cleavage state. The ribozyme folding problem was eventually solved using urea-mediated refolding, as outlined above. To trap the ribozyme in its pre-cleaved state, the catalytic cytidine was mutated to uridine, enabling ready crystallization after urea-refolding treatment. Crystals as large as $250 \times 200 \times 150\,\mu m^3$ were grown using the hanging drop vapor diffusion method over the course of two weeks at 4 °C in optimized conditions containing 5–10% (v/v) MPD, 50 mM sodium cacodylate, pH 6.0, 40–80 mM NaCl, 20 mM $MgCl_2$, and 5–15 mM spermine–HCl. Initial attempts to stabilize these crystals by increasing the MPD concentration to 30% yielded X-ray diffraction to 3.1 Å at best. A systematic screen of 36 cryoprotectants in the Hampton CryoPro kit identified sucrose as the best stabilizer. Crystals transferred stepwise into well solution plus 35% sucrose diffracted X-rays to ~2.1 Å resolution with 0.5° mosaicity. Crystals of the wild type ribozyme trapped in the precursor state by chelation of catalytic metal ion or introduction of 2′-H, MeO modification adjacent to scissile phosphate have been described in detail in the previous sections.

9. Concluding remarks

Crystallization of RNA and RNA–protein complexes remains a challenging task. While still an empirical process, the methods outlined in this review provide some systematic approaches that are applicable to a wide variety of crystallization targets. Together with exciting progress using sub-microliter sample volumes, crystallization of large and hard-to-purify RNAs and ribonucleoproteins is becoming increasingly tractable. These advances coupled with the availability and accessibility of X-ray crystallographic equipment and software will facilitate structural insights into many aspects of RNA biology that can only be elucidated through detailed molecular structure determination. For RNA structural biology, the future remains very bright indeed.

Acknowledgments

The authors thank Kaihong Zhou for excellent technical support. This work was supported in part by a grant from the NIH to J.A.D.

References

[1] M. Weselak, M. Patch, T. Selby, G. Knebel, R. Stevens, Methods Enzymol. 368 (2003) 45–76.
[2] A.R. Ferre-D'Amare, K. Zhou, J.A. Doudna, J. Mol. Biol. 279 (1998) 621–631.
[3] W.G. Scott, J.B. Murray, Methods Enzymol. 317 (2000) 180–198.
[4] J.H. Cate, J.A. Doudna, Methods Enzymol. 317 (2000) 169–180.
[5] J. Wedekind, D. McKay, Methods Enzymol. 317 (2000) 149–168.
[6] J. Wedekind, D. McKay, Nat. Struct. Biol. 6 (1999) 261–268.
[7] H. Pley, K. Flaherty, D. McKay, Nature 372 (1994) 68–74.
[8] W.G. Scott, J.T. Finch, A. Klug, Cell 81 (1995) 991–1002.
[9] R.T. Batey, R.P. Rambo, L. Lucast, B. Rha, J.A. Doudna, Science 287 (2000) 1232–1239.

[10] A.R. Ferre-D'Amare, J.A. Doudna, J. Mol. Biol. 295 (2000) 541–556.
[11] P.B. Rupert, A.R. Ferre-D'Amare, Nature 410 (2001) 780–786.
[12] A.R. Ferre-D'Amare, K. Zhou, J.A. Doudna, Nature 395 (1998) 567–574.
[13] K. Juneau, E. Podell, D. Harrington, T. Cech, Structure 9 (2001) 221–231.
[14] K. Juneau, T. Cech, Rna 5 (1999) 1119–1129.
[15] F. Guo, T. Cech, Nat. Struct. Biol. 9 (2002) 855–861.
[16] J. Milligan, D. Groebe, G. Witherell, O. Uhlenbeck, Nucleic Acids Res. 15 (1987) 8783–8798.
[17] J. Milligan, O. Uhlenbeck, Methods Enzymol. 180 (1989) 51–62.
[18] S. Price, N. Ito, C. Oubridge, J. Avis, K. Nagai, J. Mol. Biol. 249 (1995) 398–408.
[19] A.R. Ferre-D'Amare, J.A. Doudna, Nucleic Acids Res. 24 (1996) 977–978.
[20] W.G. Scott, Methods Mol. Biol. 74 (1997) 387–391.
[21] S. Chaulk, A. MacMillan, Nucleic Acids Res. 26 (1998) 3173–3178.
[22] J.B. Murray, D.P. Terwey, L. Maloney, A. Karpeisky, N. Usman, L. Beigelman, W.G. Scott, Cell 92 (1998) 665–673.
[23] B. Golden, A. Gooding, E. Podell, T. Cech, Rna 2 (1996) 1295–1305.
[24] B. Golden, Methods Enzymol. 317 (2000) 124–132.
[25] P.B. Rupert, A.P. Massey, S.T. Sigurdsson, A.R. Ferre-D'Amare, Science 298 (2002) 1421–1424.
[26] L. Bare, A. Bruce, R. Gesteland, O. Uhlenbeck, Nature 305 (1983) 554–556.
[27] M. Moore, P. Sharp, Science 256 (1992) 992–997.
[28] M. Moore, C. Query, Methods Enzymol. 317 (2000) 109–123.
[29] S. Strobel, T. Cech, Science 267 (1995) 675–679.
[30] D.M. Chadalavada, S.E. Senchak, P.C. Bevilacqua, J. Mol. Biol. 317 (2002) 559–575.
[31] D.M. Chadalavada, S.M. Knudsen, S. Nakano, P.C. Bevilacqua, J. Mol. Biol. 301 (2000) 349–367.
[32] A. Luptak, A.R. Ferre-D'Amare, K. Zhou, K.W. Zilm, J.A. Doudna, J. Am. Chem. Soc. 123 (2001) 8447–8452.
[33] S.R. Price, Chris Oubridge, Gabriele Varani, Kiyoshi Nagai, in: Smith, C.W.J. (Ed.), RNA–Protein Interactions. A Practical Approach, Oxford University Press, Oxford, 1998, pp. 37–74.
[34] J. Pan, S. Woodson, J. Mol. Biol. 280 (1998) 597–609.
[35] M. Rook, D. Treiber, J. Williamson, J. Mol. Biol. 281 (1998) 609–620.
[36] S.P. Rosenstein, M.D. Been, Biochemistry 29 (1990) 8011–8016.
[37] W.G. Scott, J.T. Finch, R. Grenfell, J. Fogg, T. Smith, M.J. Gait, A. Klug, J. Mol. Biol. 250 (1995) 327–332.
[38] J.A. Doudna, C. Grosshans, A. Gooding, C.E. Kundrot, Proc. Natl. Acad. Sci. USA 90 (1993) 7829–7833.
[39] B. Golden, E. Podell, A. Gooding, T. Cech, J. Mol. Biol. 270 (1997) 711–723.
[40] I. Berger, C. Kang, N. Sinha, M. Wolters, A. Rich, Acta Crystallogr. D Biol. Crystallogr. 1 (1996) 465–468.
[41] J. Nowakowski, P. Shim, G. Joyce, C. Stout, Acta Crystallogr. D Biol. Crystallogr. 55 (1999) 1885–1892.
[42] A. Ducruix, R.E. Giege, Oxford University Press, New York, 1992.
[43] B. Heras, M. Edeling, K. Byriel, A. Jones, S. Raina, J. Martin, Structure 11 (2003) 139–145.
[44] I.H. Shih, M.D. Been, Annu. Rev. Biochem. 71 (2002) 887–917.